

## Supporting Information

### **An octanuclear Cu(II) cluster with bio-inspired Cu<sub>4</sub>O<sub>4</sub> cubic fragment for efficient photocatalytic water oxidation**

Junqi Lin,<sup>a,‡</sup> Xiangming Liang,<sup>a,‡</sup> Xiaohu Cao,<sup>a</sup> Nannan Wei<sup>a</sup> and Yong Ding<sup>a,b\*</sup>

<sup>a</sup> *State Key Laboratory of Applied Organic Chemistry, Key Laboratory of Nonferrous Metals Chemistry and Resources Utilization of Gansu Province, College of Chemistry and Chemical Engineering, Lanzhou University, Lanzhou 730000, China*

<sup>b</sup> *State Key Laboratory for Oxo Synthesis and Selective Oxidation, Lanzhou Institute of Chemical Physics, Chinese Academy of Sciences, Lanzhou 730000, China*

‡ These authors contributed equally to this work.

\* To whom correspondence should be addressed.

E-mail addresses: dingyong1@lzu.edu.cn

## Materials

Purified water (18.2 M $\Omega$  cm) for the preparation of catalyst and buffer solutions was made by Molecular Lab Water Purifier., and all chemicals of the highest purity were obtained commercially without further purification if there was no special notification.

## Equipment and Apparatus

Infrared spectra (2 wt% in KBr pellets) were recorded using a ThermoFisher scientific Nicolet iS5 FT-IR spectrometer. UV-vis absorption spectra were recorded on Beijing Purkinje General Instrument Co.,Ltd. The capillary electrophoretic were performed on Beckman, MDQ. Equipped with a 32.karat 7.0 software. Powder X-ray diffraction (PXRD) data were collected with a PANalytical X'Pert Pro Diffractometer operated at 40 kV and 40 mA with Cu K $\alpha$  radiation (step size: 0.017 $^\circ$ , step time: 10.34 s). The capillary electrophoretic were performed on Beckman, MDQ. Equipped with a 32.karat 7.0 software. The post-reaction solutions were evaluated three times consecutively.

## Electrochemical Measurements

Cyclic voltammetry (CV) was recorded on a CHI600D electrochemical analyser with a glassy carbon, Ag/AgCl and Pt wire electrode as the working, reference and auxiliary electrodes, respectively, in buffer solutions (pH 9.0, 80 mM) at room temperature with a scanning rate of 100 mV $\cdot$ s $^{-1}$ .

## Oxygen Evolution Quantified by GC

Gas chromatography (GC) with thermal conductivity detector (TCD) has been widely used to precisely detect O $_2$  in photocatalytic water oxidation system using Ar as carrier gas.<sup>1-4</sup> We utilized GC-TCD using Ar as carrier gas to detect O $_2$  according to a method that similar to the method reported by Hill *et al.*<sup>5</sup>

Five reference volume of O $_2$  were used in constructing a multipoint calibration slope. After mixing, 0  $\mu$ L, 100  $\mu$ L, 200  $\mu$ L, 300  $\mu$ L, or 400  $\mu$ L of pure O $_2$  (corresponding to 0, 3.44, 6.89, 10.32 or 13.77  $\mu$ mol O $_2$ , the barometric pressure of Lanzhou city is 85.3 kPa) were injected into

the headspace of the reaction vessel. The reaction vessel was shaken to allow equilibration of O<sub>2</sub> between gas and aqueous phases. Contamination from air was minimal and accounted for by subtracting 1/2.81 of the nitrogen peak area from the total oxygen peak area as the gas chromatograph gives oxygen to nitrogen ratio of 1/2.81 for a sample of air. The amount of O<sub>2</sub> was plotted against the integration area for the adjusted oxygen peak. A linear correlation between the two was found and the slope was used as the conversion factor for the quantification of O<sub>2</sub> in future experiments.

For water oxidation experiments in this work, the reaction was started by irradiating the solution with a LED light source ( $\lambda = 460$  nm, 33.8 mW cm<sup>-2</sup>) at room temperature. After each sampling time, 100  $\mu$ L of Ar was injected into the flask and then the same volume of gas sample in the headspace of the flask was withdrawn by a SGE gas-tight syringe and analyzed by gas chromatography (GC). The O<sub>2</sub> in the sampled gas was separated by passing through a 2 m  $\times$  3 mm packed molecular sieve 5A column with an Ar carrier gas and quantified by a thermal conductivity detector (Shimadzu GC-9A). The total amount of evolved O<sub>2</sub> was calculated based on the concentration of O<sub>2</sub> (presented in the form of the peak area of O<sub>2</sub> detected by GC-TCD) in the headspace gas.

### **Catalyst preparation**

[Cu<sub>8</sub>(dpk·OH)<sub>8</sub>(OAc)<sub>4</sub>](ClO<sub>4</sub>)<sub>4</sub> (**1**) was synthesized according to the literature method.<sup>6</sup> A stirred blue-green solution of Cu(OAc)<sub>2</sub>·H<sub>2</sub>O (0.24 g, 1.2 mmol) in H<sub>2</sub>O (11 mL) was added to a solution of di-2-pyridyl ketone (0.22 g, 1.2 mmol) in H<sub>2</sub>O (9 mL). To the resultant blue solution an aqueous solution (10 mL) of NaClO<sub>4</sub>·H<sub>2</sub>O (0.084 g, 0.6 mmol) was added; no noticeable color change occurred. The solution was exposed to air and left for slow evaporation. Green crystals were deposited after several days and collected by filtration, washed with cold EtOH and Et<sub>2</sub>O, and dried in air (30 % yield based on Cu). Elemental analysis calculated (found) for C<sub>96</sub>H<sub>102</sub>N<sub>16</sub>O<sub>49</sub>Cl<sub>4</sub>Cu<sub>8</sub>: C, 39.56 (39.89); H, 3.53 (3.37); N, 7.69 (7.80); Cu, 17.44 (16.23).

### Catalyst characterization

**1** was authenticated by powder X-ray diffraction, elemental analysis and infrared spectroscopy. The measured powder X-ray diffraction pattern of the as-synthesized sample showed good agreement with the simulated pattern from the reported CIF of **1**, verifying the structure and high purity of the as-synthesized sample (Fig. S1). The elemental analysis coincides well with the reported data. Infrared spectrum of **1** ( $\text{cm}^{-1}$ ): 1603 (s), 1472 (m), 1443 (s), 1221 (m), 1076 (vs), 955 (m), 804 (m), 779 (m), 767 (m), 685 (m), 623 (s) (Fig. S2). Infrared spectrum is in good agreement with the reported data.<sup>1</sup>

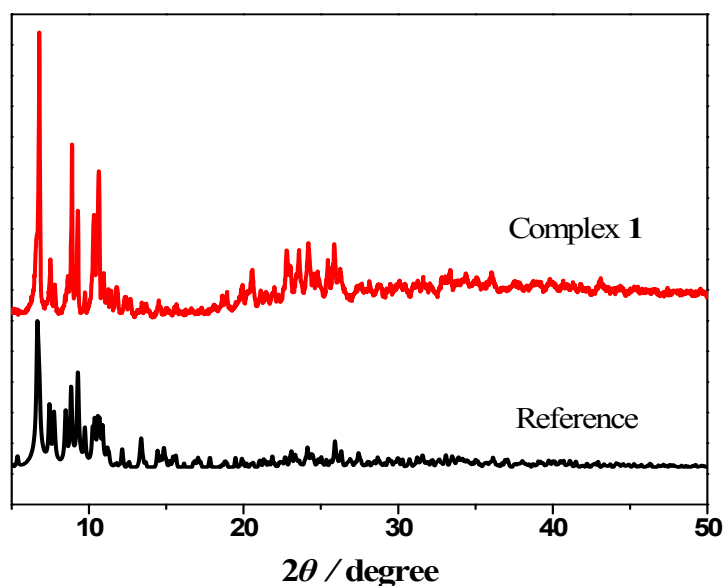


**Fig. S1** Measured (black) and simulated (blue) powder X-ray diffraction data of **1**.

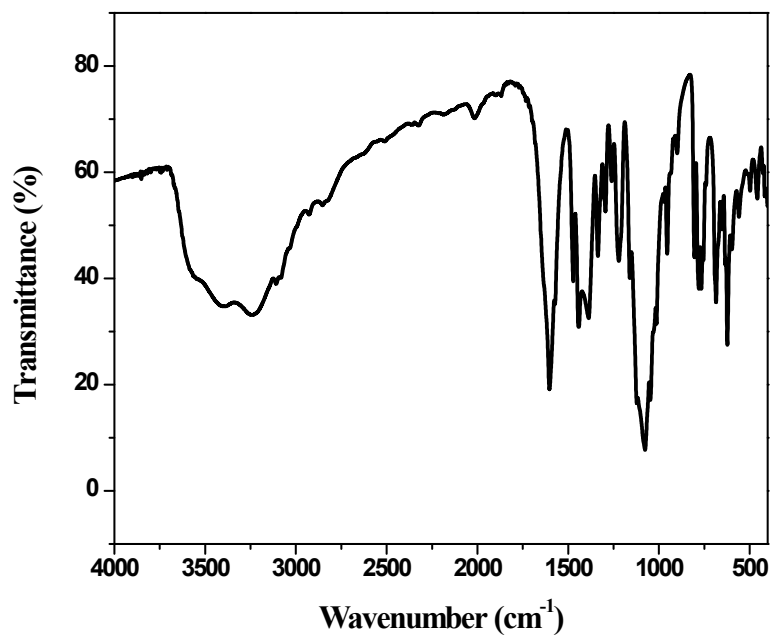


**Fig. S2** FT-IR spectrum of **1** ( $\text{cm}^{-1}$ ): 1603 (s), 1472 (m), 1443 (s), 1221 (m), 1076 (vs), 955 (m), 804 (m), 779 (m), 767 (m), 685 (m), 623 (s).

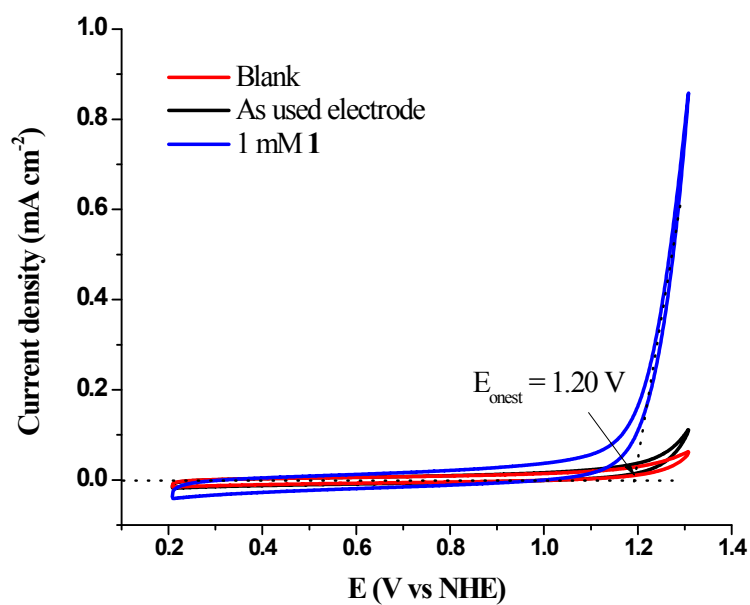


**Fig. S3** CV tests of 1 mM **1**, GC electrode and as used GC electrode in 80 mM borate buffer solution at pH 9.0 by a three-electrode system.

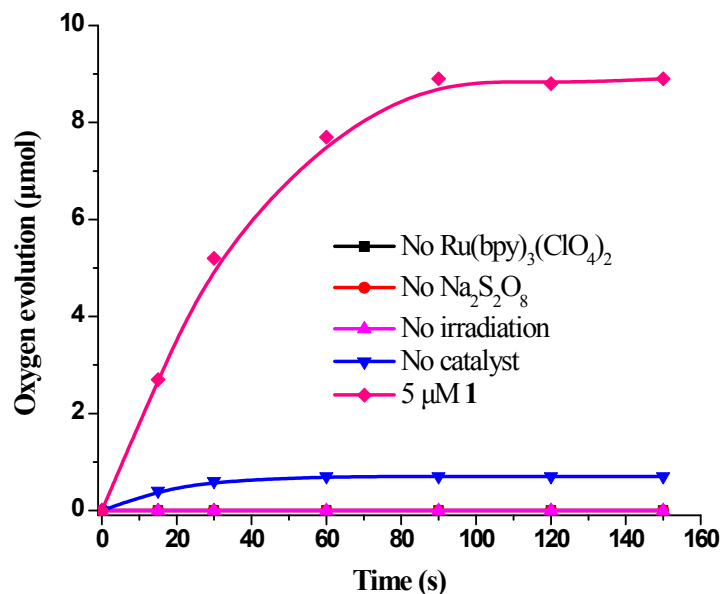


**Fig. S4** Controlled experiments of visible light-driven water oxidation catalyzed by **1** 10 mL 80 mM borate buffer solution. The concentration of  $\text{Ru}(\text{bpy})_3(\text{ClO}_4)_2$  was 0.5 mM. The concentration of  $\text{Na}_2\text{S}_2\text{O}_8$  was 5 mM.

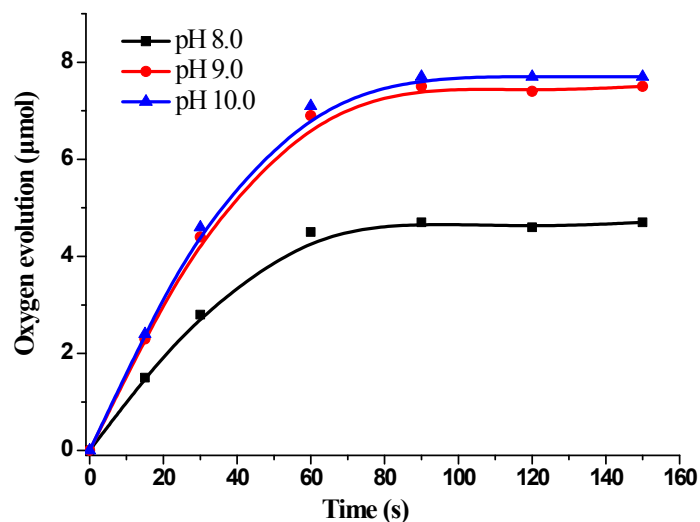


**Fig. S5** pH-dependent oxygen evolution kinetic curves, conditions: 20  $\mu\text{M}$  **1**, 1 mM  $\text{Ru}(\text{bpy})_3(\text{ClO}_4)_2$  and 5 mM  $\text{Na}_2\text{S}_2\text{O}_8$ , 10 mL 80 mM borate buffer solution at different pH. All systems were irradiated by LEDs ( $\lambda = 460 \text{ nm}$ ,  $33.8 \text{ mW cm}^{-2}$ ).

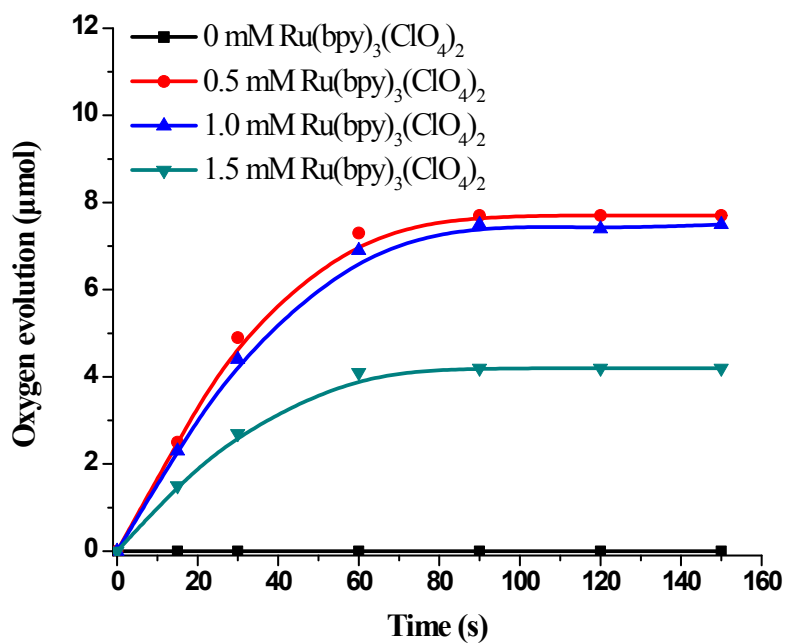


**Fig. S6** Oxygen evolution kinetic curves of different concentration of  $\text{Ru}(\text{bpy})_3(\text{ClO}_4)_2$ , conditions:  $20 \mu\text{M}$  **1** and  $5 \text{ mM}$   $\text{Na}_2\text{S}_2\text{O}_8$ ,  $10 \text{ mL}$   $80 \text{ mM}$  borate buffer solution at  $\text{pH}$   $9.0$ . All systems were irradiated by LEDs ( $\lambda = 460 \text{ nm}$ ,  $33.8 \text{ mW cm}^{-2}$ ).

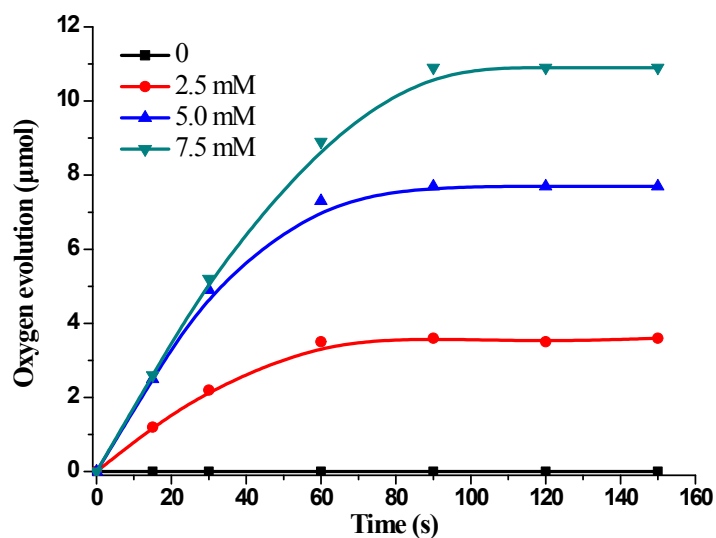


**Fig. S7** Oxygen evolution kinetic curves of different concentration of  $\text{Na}_2\text{S}_2\text{O}_8$ , conditions:  $20 \mu\text{M}$  **1** and  $0.5 \text{ mM}$   $\text{Ru}(\text{bpy})_3(\text{ClO}_4)_2$ ,  $10 \text{ mL}$   $80 \text{ mM}$  borate buffer solution at  $\text{pH}$   $9.0$ . All systems were irradiated by LEDs ( $\lambda = 460 \text{ nm}$ ,  $33.8 \text{ mW cm}^{-2}$ ).

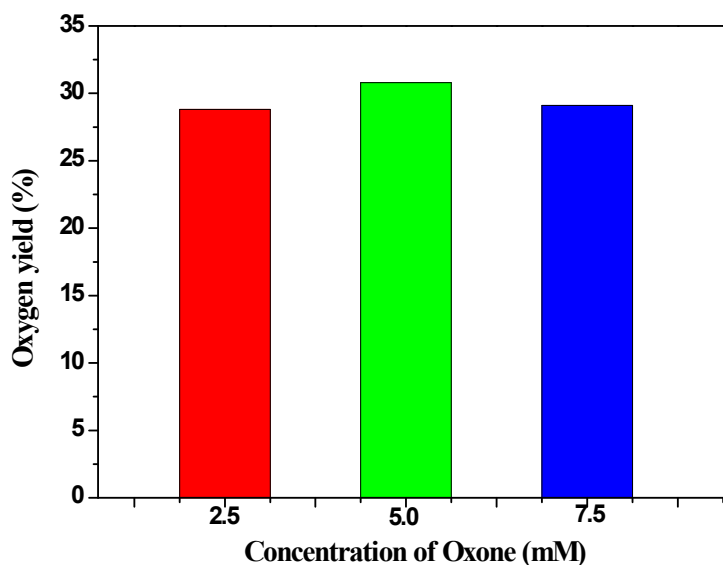


**Fig. S8** Oxygen yield of different concentration of  $\text{Na}_2\text{S}_2\text{O}_8$ , conditions: 20  $\mu\text{M}$  **1** and 0.5 mM  $\text{Ru}(\text{bpy})_3(\text{ClO}_4)_2$ , 10 mL 80 mM borate buffer solution at pH 9.0. All systems were irradiated by LEDs ( $\lambda = 460$  nm, 33.8  $\text{mW cm}^{-2}$ ).

**Table S1** Comparisons of the activity of **1** and reported Cu based homogeneous catalysts for photocatalytic water oxidation.

Catalyst	Concentration ( $\mu\text{M}$ )	Oxygen yield (%)	TON <sup>a</sup>	TOF <sup>b</sup> ( $\text{s}^{-1}$ )	Ref
<b>1</b> <sup>c</sup>	5	35.6	178	3.6	This work
$\text{Cu}_5\text{-POM}^d$	20	18.3	23	0.15	7
$\text{Cu}(\text{F}_3\text{TPA})(\text{ClO}_4)_2$ <sup>e</sup>	30	13.9	11.6	0.16	8
$\text{CuPcTS}^f$	20	14.9	26	0.063	9
$[\text{Cu}(\text{tza})_2]_n^g$	5	10.3	25.76	1.68	10

<sup>a</sup> TON = mole of oxygen/mole of catalyst. <sup>b</sup> TOF = TON(initial 15 s)/15 s. <sup>c</sup> 0.5 mM  $\text{Ru}(\text{bpy})_3(\text{ClO}_4)_2$ , 5 mM  $\text{Na}_2\text{S}_2\text{O}_8$ , 10 mL 80 mM borate buffer solution at pH 9.0, LEDs ( $\lambda = 460$  nm, 33.8  $\text{mW cm}^{-2}$ ). <sup>d</sup>  $\text{Cu}_5\text{-POM} = [\text{Cu}_5(\text{OH})_4(\text{H}_2\text{O})_2(\text{A-}\alpha\text{-SiW}_9\text{O}_{33})_2]^{10-}$ , 1 mM  $\text{Ru}(\text{bpy})_3\text{Cl}_2$ , 5 mM  $\text{Na}_2\text{S}_2\text{O}_8$ , borate buffer solution at pH 9.0, LEDs ( $\lambda \geq 420$  nm, 16  $\text{mW cm}^{-2}$ ). <sup>e</sup> 0.4 mM  $\text{Ru}(\text{bpy})_3(\text{ClO}_4)_2$ , 5 mM  $\text{Na}_2\text{S}_2\text{O}_8$ , borate buffer solution at pH 8.5, LEDs ( $\lambda = 470$  nm, 820  $\mu\text{Ecm}^{-2} \text{s}^{-1}$ ). <sup>f</sup> 0.2 mM  $\text{Ru}(\text{bpy})_3(\text{NO}_3)_2$ , 7 mM  $\text{Na}_2\text{S}_2\text{O}_8$ , borate buffer solution at pH 9.5, 300 W Xe (400-800 nm). <sup>g</sup> 1 mM  $\text{Ru}(\text{bpy})_3\text{Cl}_2$ , 2.5 mM  $\text{Na}_2\text{S}_2\text{O}_8$ , borate buffer solution at pH 9.0. LEDs ( $\lambda = 450$  nm).



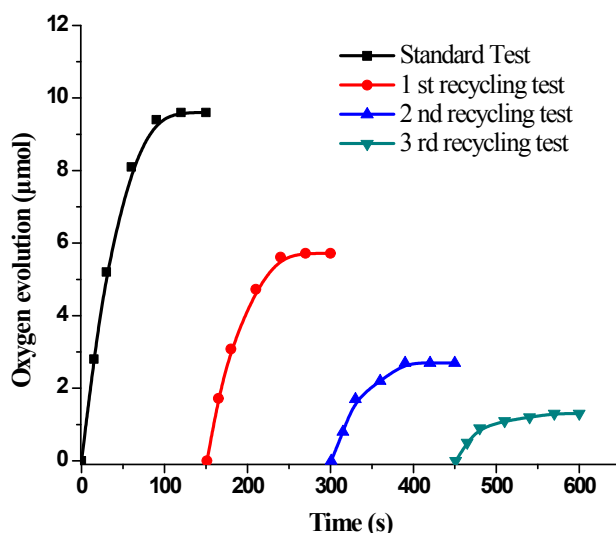


**Fig. S9** Recycling photocatalytic test of **1** (10  $\mu\text{M}$ ) with addition of  $\text{Na}_2\text{S}_2\text{O}_8$  in 80 mM borate buffer solution at pH 9.0. Conditions for the standard test (black): 0.5 mM  $[\text{Ru}(\text{bpy})_3](\text{ClO}_4)_2$  and 5 mM  $\text{Na}_2\text{S}_2\text{O}_8$ . The first recycling test (red) was performed by adding 5 mM  $\text{Na}_2\text{S}_2\text{O}_8$  to the standard test solution after readjusting the pH of the post-catalytic solution to 9.0. The second recycling test (blue) started from the adjustment of the first recycled solution to pH 9.0 and addition of 5 mM  $\text{Na}_2\text{S}_2\text{O}_8$ . The third recycling test (cyan) started from the adjustment of the second recycled solution to pH 9.0 and addition of 5 mM  $\text{Na}_2\text{S}_2\text{O}_8$ . All reaction reaction solutions were irradiated by LEDs ( $\lambda = 460 \text{ nm}$ ,  $33.8 \text{ mW cm}^{-2}$ ).

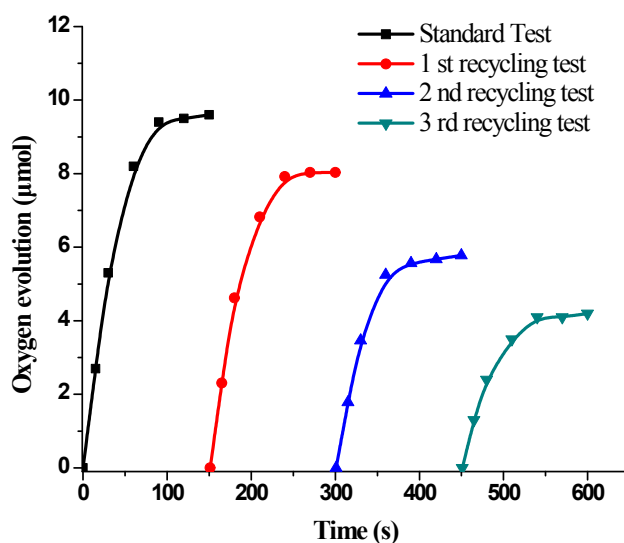


**Fig. S10** Recycling photocatalytic test of **1** (10  $\mu\text{M}$ ) with addition of  $[\text{Ru}(\text{bpy})_3](\text{ClO}_4)_2$  and  $\text{Na}_2\text{S}_2\text{O}_8$  in 80 mM borate buffer solution at pH 9.0. Conditions for the standard test (black): 0.5 mM  $[\text{Ru}(\text{bpy})_3](\text{ClO}_4)_2$ , 5 mM  $\text{Na}_2\text{S}_2\text{O}_8$ . The first recycling test (red) was performed by adding 0.5 mM  $[\text{Ru}(\text{bpy})_3](\text{ClO}_4)_2$  and 5 mM  $\text{Na}_2\text{S}_2\text{O}_8$  to the standard test solution after readjusting the pH of the post-catalytic solution to 9.0. The second recycling test (blue) started from the adjustment of the first recycled solution to pH 9.0 and addition of 0.5 mM  $[\text{Ru}(\text{bpy})_3](\text{ClO}_4)_2$  and 5 mM  $\text{Na}_2\text{S}_2\text{O}_8$ . The third recycling test (cyan) started from the adjustment of the second recycled solution to pH 9.0 and addition of 0.5 mM  $[\text{Ru}(\text{bpy})_3](\text{ClO}_4)_2$  and 5 mM  $\text{Na}_2\text{S}_2\text{O}_8$ . All reaction reaction solutions were irradiated by LEDs ( $\lambda = 460 \text{ nm}$ ,  $33.8 \text{ mW cm}^{-2}$ ).

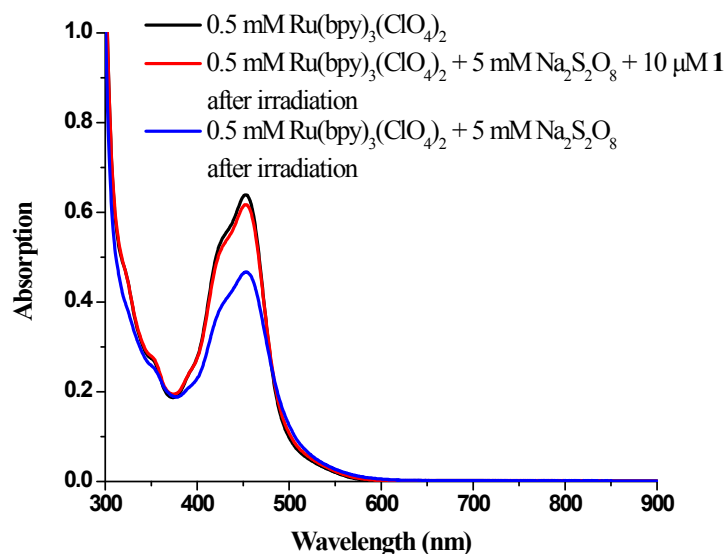


**Fig. S11** UV-vis absorption spectrum of 0.5 mM  $[\text{Ru}(\text{bpy})_3](\text{ClO}_4)_2$  in 10 mL pH 9.0 borate buffer solution (black trace), 0.5 mM  $[\text{Ru}(\text{bpy})_3](\text{ClO}_4)_2 + 5 \text{ mM Na}_2\text{S}_2\text{O}_8 + 10 \mu\text{M } \mathbf{1}$  in pH 9.0 borate buffer solution after irradiation (red trace) and 0.5 mM  $[\text{Ru}(\text{bpy})_3](\text{ClO}_4)_2 + 5 \text{ mM Na}_2\text{S}_2\text{O}_8$  in pH 9.0 borate buffer solution after irradiation (blue trace). LEDs ( $\lambda = 460 \text{ nm}$ ,  $33.8 \text{ mW cm}^{-2}$ ) was used as light source.

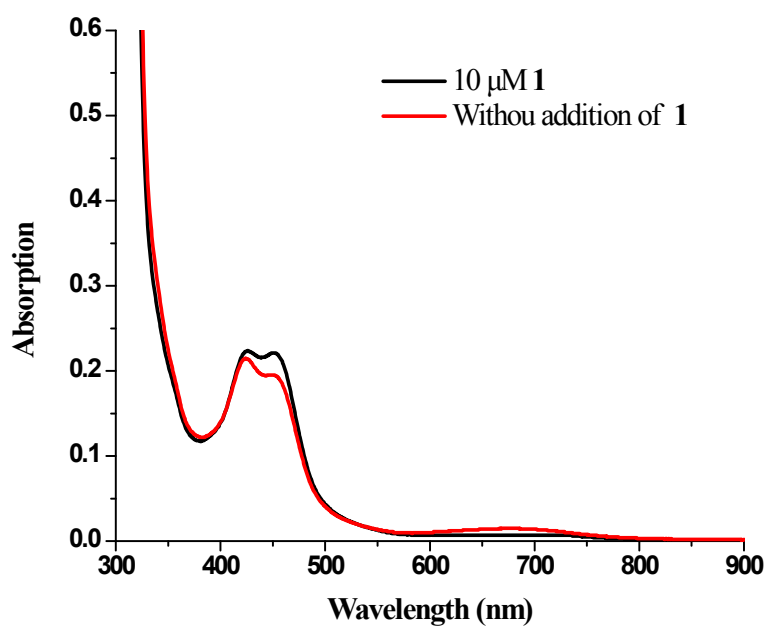


**Fig. S12** UV-vis absorption spectrum of 0.5 mM  $[\text{Ru}(\text{bpy})_3](\text{ClO}_4)_2 + 5 \text{ mM Na}_2\text{S}_2\text{O}_8 + 10 \mu\text{M } \mathbf{1}$  in pure water after irradiation (black trace) and 0.5 mM  $[\text{Ru}(\text{bpy})_3](\text{ClO}_4)_2 + 5 \text{ mM Na}_2\text{S}_2\text{O}_8$  in pure water after irradiation (red trace). LEDs ( $\lambda = 460 \text{ nm}$ ,  $33.8 \text{ mW cm}^{-2}$ ) was used as light source.

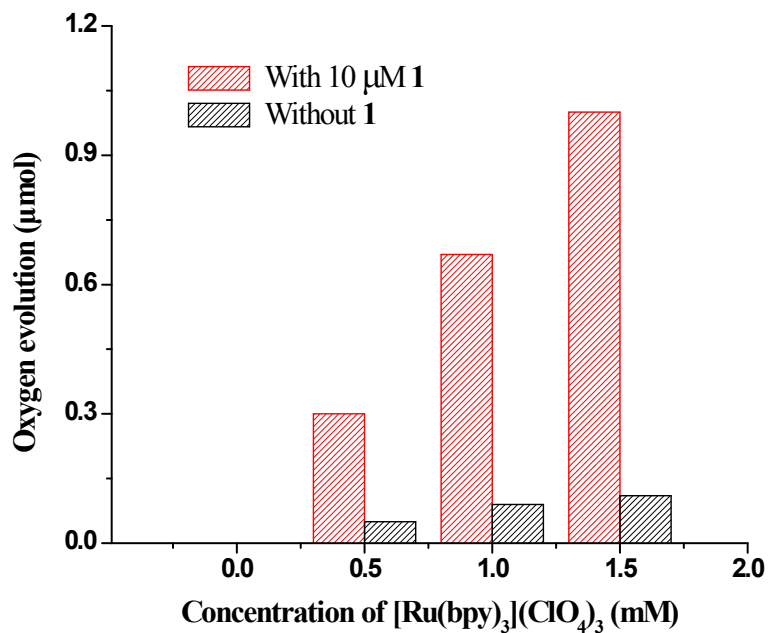


**Fig. S13** Oxygen evolution amount of chemical water oxidation by various concentration of [Ru(bpy)<sub>3</sub>](ClO<sub>4</sub>)<sub>3</sub> with or without 10 μM **1** in 10 mL 80 mM borate buffer solution at pH 9.0.

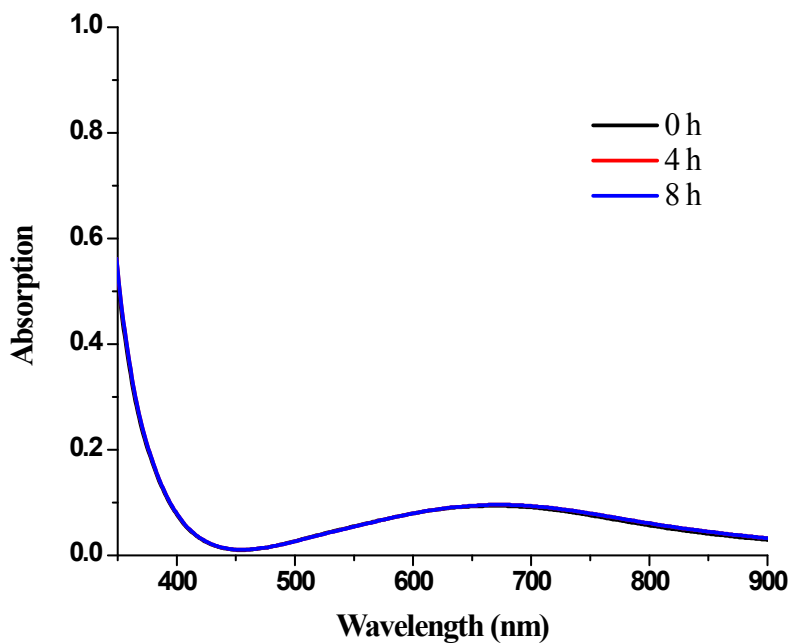


**Fig. S14** Time-independent UV-vis spectra of **1** in 80 mM borate buffer solution at pH 9.0.

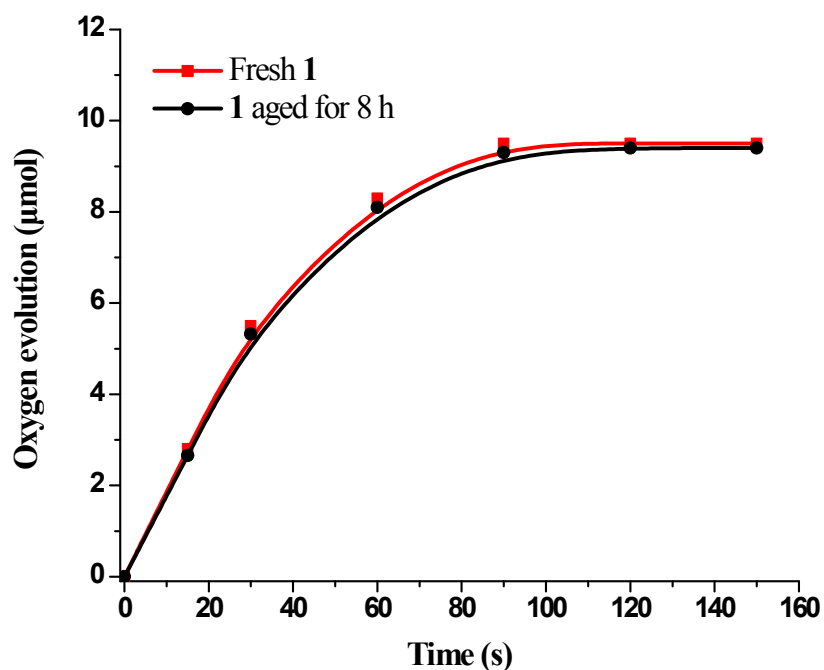


**Fig. S15** Oxygen evolution kinetic curves of catalyzed by fresh  $20 \mu\text{M}$  **1** and  $20 \mu\text{M}$  **1** aged for 8 h. Conditions:  $0.5 \text{ mM Ru}(\text{bpy})_3(\text{ClO}_4)_2$ ,  $10 \text{ mL } 80 \text{ mM}$  borate buffer solution at pH 9.0. All systems were irradiated by LEDs ( $\lambda = 460 \text{ nm}$ ,  $33.8 \text{ mW cm}^{-2}$ ).

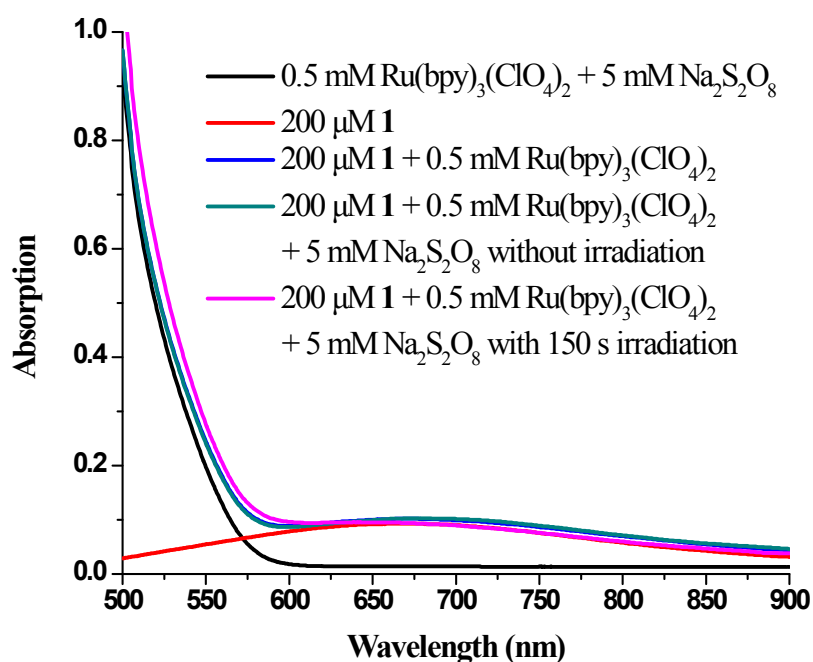


**Fig. S16** UV-vis spectra of the reaction solution containing  $200 \mu\text{M}$  **1** before and after reaction.

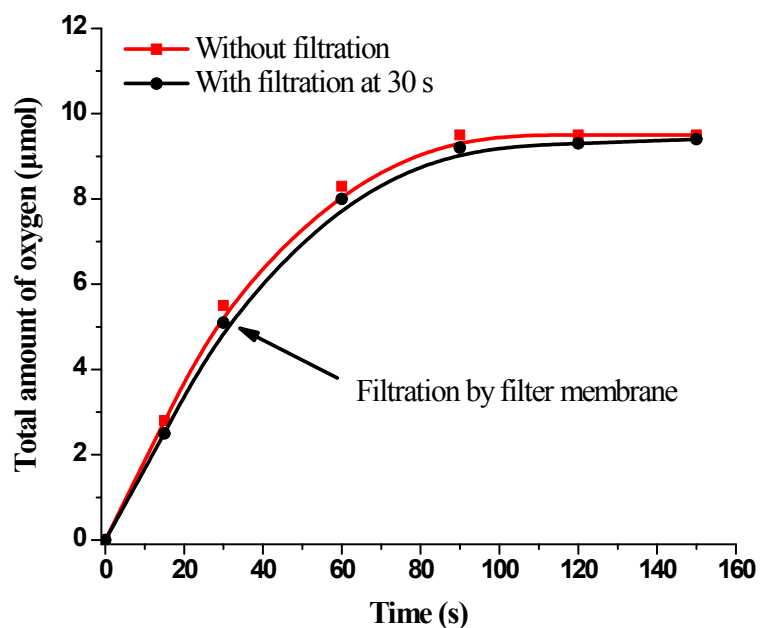


**Fig. S17** Kinetic curves of visible light-driven water oxidation catalyzed by 10  $\mu\text{M}$  **1** in 10 mL 80 mM borate buffer solution at pH 9.0. (Black curve) The solution was not filtered by filter membrane. (Red) The reaction solution was filtered by a filter membrane at 30 s.

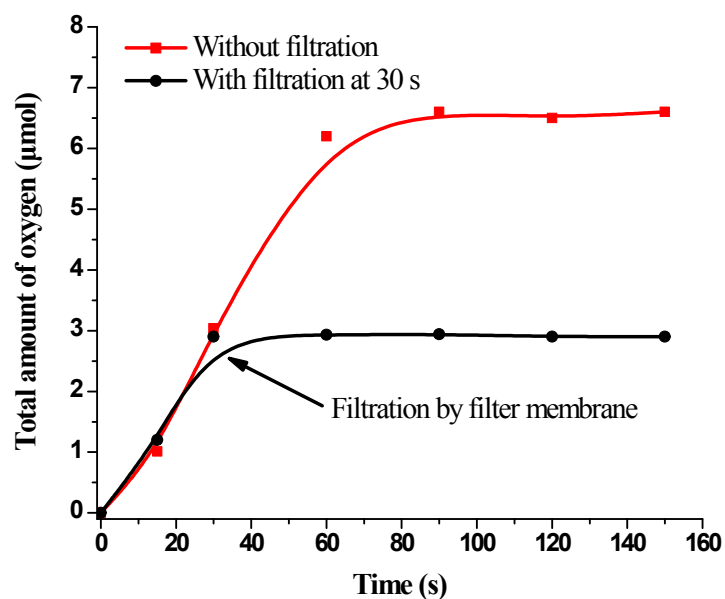


**Fig. S18** Kinetic curves of visible light-driven water oxidation catalyzed by 10  $\mu\text{M}$   $\text{Cu}^{2+}$  in 10 mL 80 mM borate buffer solution at pH 9.0. (Black curve) The solution was not filtered by filter membrane. (Red) The reaction solution was filtered by a filter membrane at 30 s.

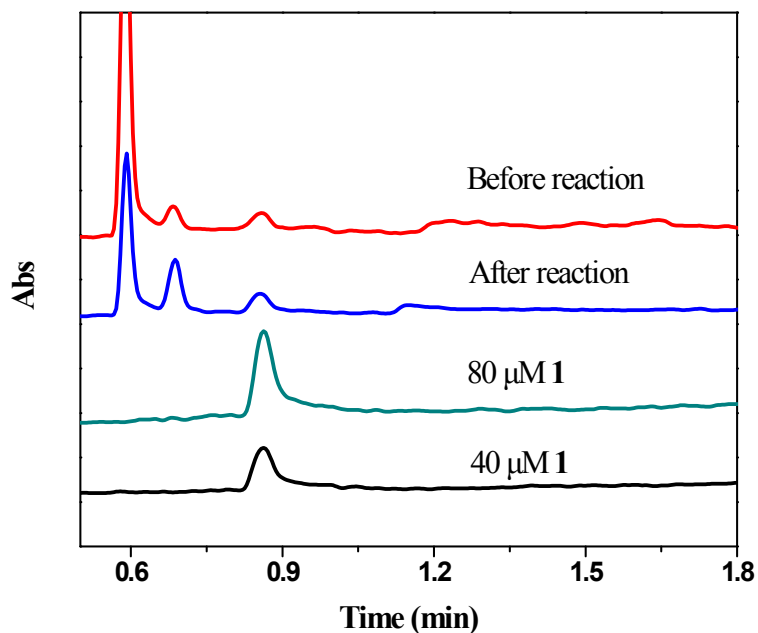


**Fig. S19** An electropherogram for **1**. Black line: 40  $\mu\text{M}$  of **1** in a 20 mM sodium borate buffer solution at pH 9.0. Cyan line: 80  $\mu\text{M}$  of **1** in 10 mL 20 mM sodium borate buffer solution at pH 9.0. Blue line: 20  $\mu\text{M}$  of **1** in a 20 mM sodium borate buffer solution at pH = 9.0 containing  $[\text{Ru}(\text{bpy})_3](\text{ClO}_4)_2$  (0.5 mM),  $\text{Na}_2\text{S}_2\text{O}_8$  (5.0 mM) after 150 s of illumination. Experimental conditions for capillary electrophoresis: Fused-silica capillaries (75  $\mu\text{m}$  i.d., 365  $\mu\text{m}$  o.d., Hebei Yongnian Factory, China) with total length of 50.2 cm and effective length of 10 cm were used. The detection wavelength was set at 214 nm. The running buffer for CE separation was 20 mM sodium borate buffer (pH 10.0). The separation voltage was set at -20 kV. The sample was injected into the capillary (0.5psi, 3 s).

## Reference

- 1 Y. V. Geletii, Z. Huang, Y. Hou, D. G. Musaev, T. Lian and C. L. Hill, *J. Am. Chem. Soc.*, 2009, **131**, 7522.
- 2 D. Hong, Y. Yamada, T. Nagatomi, Y. Takai and S. Fukuzumi, *J. Am. Chem. Soc.*, 2012, **134**, 19572.
- 3 T. Zhou, D. Wang, S. Chun-Kiat Goh, J. Hong, J. Han, J. Mao and R. Xu, *Energy Environ. Sci.*, 2015, **8**, 526.
- 4 M. Murakami, D. Hong, T. Suenobu, S. Yamaguchi, T. Ogura and S. Fukuzumi, *J. Am. Chem. Soc.*, 2011, **133**, 11605.
- 5 Q. Yin, J. M. Tan, C. Besson, Y. V. Geletii, D. G. Musaev, A. E. Kuznetsov, Z. Luo, K. I. Hardcastle and C. L. Hill, *Science*, 2010, **328**, 342.
- 6 V. Tangoulis, C. P. Raptopoulou, A. Terzis, S. Paschalidou, S. P. Perlepes and E. G. Bakalbassis, *Inorg. Chem.*, 1997, **36**, 3996.
- 7 L. Yu, X. Du, Y. Ding, H. Chen and P. Zhou, *Chem. Commun.*, 2015, **51**, 17443.
- 8 R.-J. Xiang, H.-Y. Wang, Z.-J. Xin, C.-B. Li, Y.-X. Lu, X.-W. Gao, H.-M. Sun and R. Cao, *Chem. Eur. J.*, 2016, **22**, 1602.

- 9 R. Terao, T. Nakazono, A. R. Parent and K. Sakai, *ChemPlusChem*, 2016, **81**, 1064.
- 10 X. Jiang, B. Yang, Q.-Q. Yang, C.-H. Tung and L.-Z. Wu, *Chem. Commun.*, 2018, **54**, 4794.